GEOLOGY OF RUBY RIDGE, SOUTHWESTERN BROOKS RANGE, ALASKA

By W.G. Gilbert, M.A. Wiltse, J.R. Carden, R.B. Forbes, and S.W. Hackett

---

GEOLOGIC REPORT 58

STATE OF ALASKA

Jay S. Hammond, *Governor*

Robert E. LeResche, *Commissioner, Dept. of Natural Resources*

Ross G. Schaff, *State Geologist*

Cover photo: Helecitic garnet in glaucophane-bearing metabasalt from Ruby Ridge (X46).

For sale by Alaska Division of Geological and Geophysical Surveys, P.O. Box 80007, College, 99708; 3327 Fairbanks St., Anchorage, 99503; P.O. Box 2438, Ketchikan, 99901; and Pouch M, Juneau, 99811.

CONTENTS

ILLUSTRATIONS

TABLE

GEOLOGY OF RUBY RIDGE, SOUTHWESTERN BROOKS RANGE, ALASKA

By W.G. Gilbert,[1] M.A. Wiltse,[2] J.R. Carden,[3] R.B. Forbes,[3] and S.W. Hackett[1]

ABSTRACT

Ruby Ridge contains a polymetamorphic assemblage of pelitic schist and lesser amounts of metabasite, metafelsite, and marble. Pelitic schist is generally muscovite-quartz schist but includes chloritoid-bearing, graphitic, and calcareous units. Metabasite lenses within the pelitic schist vary between glaucophane-bearing and greenschist varieties. Most of the pelitic schist, marble, and metabasite was metamorphosed in the blueschist facies in late Precambrian time. The metafelsite generally contains biotite and microcline and is either of mid-Paleozoic or Cretaceous age. Weakly metamorphosed rocks on the tip of the ridge are probably either continuous with Paleozoic rocks in the Cosmos Hills or are the low-grade part of a progressively metamorphosed terrane.

Greenschist-facies metamorphic segregation, thrust faults, and isoclinal to subisoclinal folds overturned to the north developed during widespread Cretaceous tectonism and plutonism. Open to subisoclinal folds, slip cleavage, and, perhaps, the Kalurivik Arch formed during Late Cretaceous or Tertiary time.

Linear zones of high magnetic intensity lie over the Cosmos Hills and uplands of the Baird and Schwatka Mountains. Broad magnetic lows and highs occur over the southern portion of the schist belt, and flat magnetic lows occur over the Ambler Lowland. The aeromagnetic evidence suggests that the tectonic boundary between the Cosmos Hills-Angayucham terrane and the schist belt was reactivated as a strike-slip system during Tertiary time.

INTRODUCTION

PURPOSE AND SCOPE

This study is the result of cooperative efforts between the Alaska Division of Geological and Geophysical Surveys (DGGS), the U.S. Geological Survey, and the University of Alaska to obtain detailed information on the structure, petrology, and mineral deposits of the southern Brooks Range schist belt. In 1973, Forbes, Gilbert, and Carden began a reconnaissance study of the ridge containing VABM Ruby—hereinafter referred to as "Ruby Ridge"—and Gilbert and Wiltse completed the geologic traverse in 1975. Field work was accomplished by foot traverses from helicopter-supported base camps. The geology along Ruby Ridge, petrography of approximately 100 thin sections, and results of an aeromagnetic survey of the west-central Brooks Range by Hackett are summarized in this report.

PREVIOUS WORK

Fritts (1969, 1970) reported on the geology and mineralization of the Cosmos Hills, located south of Ruby Ridge, and of the Angayucham Mountains in the northwestern Hughes quadrangle (Fritts, 1971). Results of the Alaska DGGS field studies in the southwestern Survey Pass quadrangle were reported by Fritts and others (1972). Forbes and others (1974) presented preliminary results of the traverse along Ruby Ridge and listed metamorphic mineral assemblages encountered. Pessel and others (1973a,b), Pessel and Brosge (1977), and Brosge and Pessel (1977) have summarized the regional geology of the southern Brooks Range. Turner (1974) and Turner and Forbes (1977) reported on geochronology of metamorphic rocks collected from the schist belt.

GEOLOGIC SETTING

Ruby Ridge, located in the northern part of the Ambler River A-2 quadrangle and southern part of the Ambler River B-2 quadrangle, extends from the end of the ridge 9.0 km north of the settlement of Bornite northeast for about 26 km (fig. 1). The ridge is within the western Brooks Range schist belt as defined by Fritts and others (1972), Pessel and others (1973b), Pessel and Brosge (1977), and Brosge and Pessel (1977) (fig. 1). The schist belt contains pelitic, psammitic, and calcareous medisediments and metaigneous rocks, metamorphosed to prehnite-pumpellyite, blueschist, and greenschist facies. Mica-quartz schist and metabasite are the most conspicuous rocks in the belt. The schist belt is largely separated from extensive limestone, calcareous schist, and Cretaceous intrusive terranes to the north by the Walker Lake lineament (Fritts and others, 1972; Pessel and others, 1973a,b). The southern margin of the schist belt generally forms the north side of the Ambler Lowland (fig. 1).

The metamorphic history of the schist belt is com-

[1]Alaska Division of Geological and Geophysical Surveys, College, AK 99708.
[2]Pacific Cordillera Exploration, SRA 20826, Fairbanks, AK 99701.
[3]Solid-Earth Sciences Program, College of Environmental Sciences, University of Alaska, Fairbanks, AK 99701.

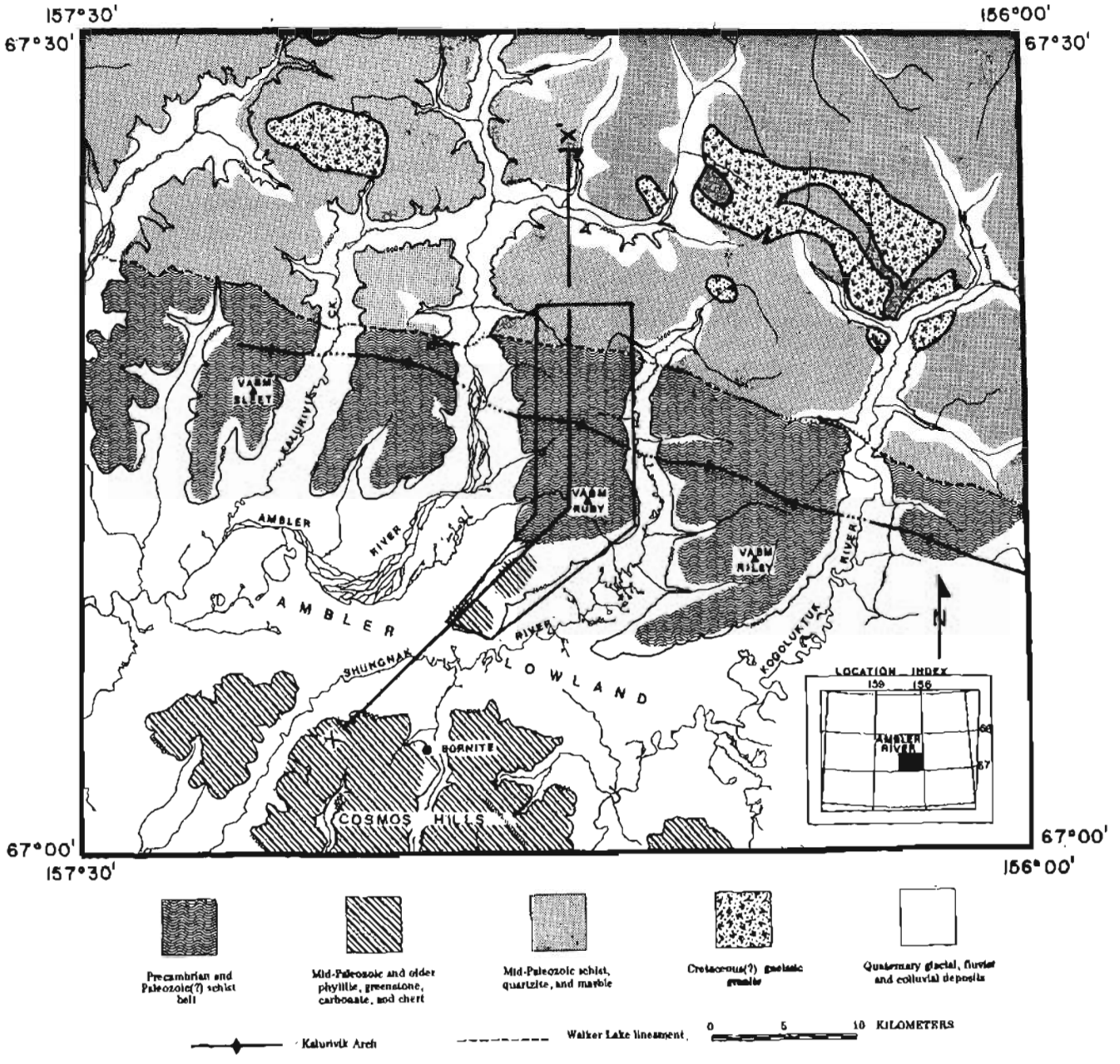

Figure 1. General geology and location of study area. X-X' shown in fig. 17.

plex and not completely documented. Potassium-argon ($^{40}K/^{40}Ar$) ages derived from the schist-belt on metabasite and quartz-mica schist suggest that some schist-belt rocks may be Precambrian (Turner, 1974; Turner and Forbes, 1977). A Cretaceous regional thermal event associated with emplacement of granitic plutons is also suggested by radiometric ages (Patton and others, 1968; Turner, 1974; Mayfield, 1975; Turner and Forbes, 1977). The thermal pulse associated with the intrusion of Cretaceous plutons may have locally reset $^{40}K/^{40}Ar$ ages for considerable distances around the larger intrusions.

Some rocks in the schist belt, however, may be equivalent in age to metamorphic units of the Angayucham Mountains-Cosmos Hills to the south (Wiltse and Gilbert, 1977) (fig. 1). Devonian(?) fossils are reported by Brosge and Pessel (1977) from a marble interval in the schist belt 42 km east of Ruby Ridge. Marbles yielding Devonian fossils have also been reported from metabasite-bearing sequences in the Cosmos Hills (Fritts, 1970) and the Angayucham Mountains (Patton and others, 1968; Fritts and others, 1972). The Angayucham

basalt may be in part Permian in age as suggested by fossils reported by Patton and Miller (1973) from correlative units in the central Brooks Range. Proponents of a Permian age for the Angayucham Mountains (and by extension, the metabasite of the Brooks Range schist belt) suggest that the Devonian(?) or older carbonate of both areas was emplaced tectonically by thrust faulting or by infolding (Tailleur, pers. comm.).

The most pronounced structure along the schist belt is a large antiform, the Kalurivik Arch (Pessel and others, 1973a). Several west-trending antiformal upwarps, including the Kalurivik Arch, which persist from the Redstone and Shishakshinovick plutons on the north to the core of the eastern Cosmos Hills on the south (Pessel and others, 1973b; Fritts, 1971), may have formed by uparching during emplacement of Cretaceous plutons.

East of the map area the Walker Lake lineament is thought to be a regional thrust fault separating the schist belt on the south from a carbonate-rich terrane to the north (Fritts and others, 1972; Pessel and others, 1972a,b). The fault may die out to the west as an unconformity (Pessel, pers. comm.).

The Ambler Lowland is thought to be the locus of a thrust fault (Fritts and others, 1972) or of a synclinal trough (Pessel and others, 1973b).

PETROLOGY

INTRODUCTION AND AGE OF ROCK UNITS

The rocks exposed on Ruby Ridge are dominately a polymetamorphic assemblage of quartz-rich pelitic schist and lesser amounts of marble, metabasite, and metafelsite. The different rock types commonly occur together, but the marble and metabasite are most abundant near VABM Ruby and near peak 3870 on the north end of the ridge, and the metafelsite is exposed only near VABM Ruby (pl. 1).

Metapelite and metabasite exhibit effects of at least two periods of regional dynothermal metamorphism. The first metamorphic event recrystallized the rocks in the blueschist facies and a second thermal event, more intense to the north, partially or completely recrystallized these rocks in the greenschist facies. The metafelsite appears to have been affected by only the second event.

Radiometric evidence (Turner, 1974; Turner and Forbes, 1977) indicates that most of the intercalated pelitic schist, marble, and metabasite on Ruby Ridge represents Precambrian basement. However, workers who have studied the metafelsite do not agree on its origin and age. Authors Wiltse and Gilbert believe the metafelsite represents felsic volcanic rocks of probable mid-Paleozoic age that unconformably overlie Precambrian basement and are now tectonically intercalated with it, whereas authors Forbes and Carden suggest that the metafelsite on Ruby Ridge represents hypabyssal apophyses of Cretaceous granitic intrusions that were emplaced synkinematically during the second major metamorphic event.

Weakly metamorphosed phyllite, metabasalt, and marble crop out on the low, southwesternmost part of Ruby Ridge (pl. 1). These rocks are probably either continuous with Paleozoic(?) rocks in the Cosmos Hills to the south rather than with the main part of the schist belt to the north (Gilbert, Wiltse, and Carden), or are the low-grade part of a progressively metamorphosed terrane that increases in grade to the north (Forbes).

PELITIC SCHIST

Brown-weathering muscovite-quartz schist volumetrically dominates the rocks exposed on Ruby Ridge. The schist is fine to medium grained and rarely contains large porphyroblasts of albite or garnet. Schistosity is defined by the parallel alignment of chlorite and white mica, and a second S surface defined by slip cleavage parallel to axial surfaces of small crenulations is occasionally present.

Quartz and muscovite are the dominant minerals in the pelitic schist, although chloritoid, graphite, chlorite, calcite, garnet, and albite occur locally. Trace amounts of sphene and apatite are nearly ubiquitous.

Chloritoid-bearing mica schist occurs in irregular east-west-trending horizons several meters thick near VABM Ruby. These rocks contain quartz, muscovite, chloritoid, graphite, glaucophane, and chlorite, trace amounts of albite, and small (1-mm-dia) garnet porphyroblasts. Similar schist is found on a ridge 8-10 km southeast of VABM Ruby and near the north end of Ruby Ridge, where a chlorite-bearing chloritoid-biotite-muscovite quartz schist is present. Chloritoid-bearing mica schist exhibits well-segregated, crenulated layers of muscovite and chloritoid separated by bands of fine-grained quartz; except for the presence of chloritoid and glaucophane, the schist is similar to "normal" mica-quartz pelitic schist. Chloritoid probably crystallized at the same time as muscovite. Small patches of pennine chlorite are scattered throughout the muscovite-chloritoid layers. Chlorite rarely truncates or transects muscovite, but more commonly precedes muscovite in the paragenetic sequence. Albite is rare in chloritoid-bearing rocks, and small (1.5-mm dia), colorless to orange, skeletal to euhedral garnet is rare. The garnet formed late in the paragenetic sequence.

Lenses of black graphitic schist up to several meters thick are scattered throughout the pelitic schist. Outcrops of graphitic schist may be bold and well jointed or subdued and covered with thin slabby talus, depending on the relative abundance of quartz. Graphitic schist consists of quartz + muscovite + graphite $\pm$ phengite $\pm$ talc $\pm$ albite $\pm$ chlorite $\pm$ calcite, and trace amounts of sphene. Muscovite-phengite is universally

present, and occasionally felted masses of talc(?) are observed in graphitic schist associated with known ore horizons. Albite, when present, occurs as porphyroblasts that have totally or partially replaced the other minerals. Minor calcite and chlorite occasionally are present in albite-bearing graphitic schist.

North of VABM Ruby some schist horizons have enough calcite to be designated calcareous schist. These rocks are essentially chlorite-muscovite-quartz schist that contains several percent calcite. They tend to be associated with thin, discontinuous marble units.

A few pelitic schist intervals immediately north of VABM Ruby are composed of white to greenish-white, intensely crenulated, quartz-muscovite talc schist. Fine- to medium-grained quartz and muscovite-phengite dominate this white schist. The presence of talc is indicated by a slight greasy feel on schistosity surfaces and by felted aggregates of a very fine-grained phyllosilicate occasionally observed as patches associated with muscovite. Minor albite, pennine, and calcite are occasionally present in the white schist and occur late in its paragenesis. Sphene is present in trace amounts.

Green and white chlorite-muscovite-albite-quartz schist containing abundant poikiloblastic albite porphyroblasts crops out on the north end of Ruby Ridge. These rocks, which may be younger than the Precambrian(?) pelitic rocks to the south, form part of a Paleozoic sequence continuing to the north.

MARBLE

Discontinuous marble lenses up to 300 m thick form a conspicuous but minor part of the rock assemblage near VABM Ruby. More continuous beds of marble up to 440 m thick are found along the north part of the ridge and appear to be the southern edge of a major Paleozoic carbonate terrane that continues to the north (pl. 1).

The marble is gray weathering, gray on a fresh surface, and ranges from fine- to medium-grained crystalloblastic marble to thinly laminated, highly contorted schistose marble with an appreciable amount of silicate minerals. The latter lithology represents a transition from calcareous schist to marble. The marble consists dominantly of calcite, but minor quartz grains are scattered throughout, as are chlorite and muscovite. Sparse, irregular porphyroblasts of albite are present in some specimens. The marble lenses probably represent premetamorphic limestone beds.

METABASITE

Greenstone lenses are prominant along Ruby Ridge, especially near VABM Ruby (fig. 2) and in the tectonically thickened zone near peak 3870 (pl. 1). The metabasite forms lensoid pods and layers up to 500 m thick and several hundred meters long parallel to the

Figure 2. Looking northwest from VABM Ruby. Dark areas are glaucophane-bearing metabasite.

dominant foliation (S_1); it rarely occurs as bodies up to several meters thick that cut across the dominant foliation. Exposures range from massive, jointed, angular outcrops surrounded by large, blocky boulders to well-foliated, schistose-slabby outcrops. The metabasite interval on the crest of Ruby Ridge 1.7 km north of VABM 3870 has pillow structures. The parent material of the metabasite probably consisted of basalt flows and gabbroic intrusions (table 1).

There is a continuous variation between massive, coarse-grained, glaucophane-bearing metabasite and occasionally foliated, fine- to medium-grained greenstone with greenschist-facies mineral assemblages (figs. 3, 4, and 5), but the two end members will be described separately.

GLAUCOPHANE-BEARING METABASITE

These rocks are generally massive with no apparent schistosity and form prominent ridges (fig. 2). Fresh samples are blue to bluish green, with a coarse-grained, poikioblastic granular texture highlighted by reddish-brown garnets that stand out in relief on weathered surfaces. The absence of schistosity, which is unusual for glaucophane schist, appears to be due to the lack of penetrative deformation. However, a crude foliation was observed in a few partially retrograded rocks and appears to be defined by minerals such as chlorite, actinolite, and white mica that crystallized during the later greenschist-facies event. A notable exception is a metabasite near the axis of the Kalurivik Arch that has a well-defined schistosity defined by the parallel alignment of subidioblastic glaucophane prisms.

The main metamorphic minerals present in glaucophane-bearing metabasite are garnet, glaucophane, epidote, sphene, rutile, chlorite, and white mica. This

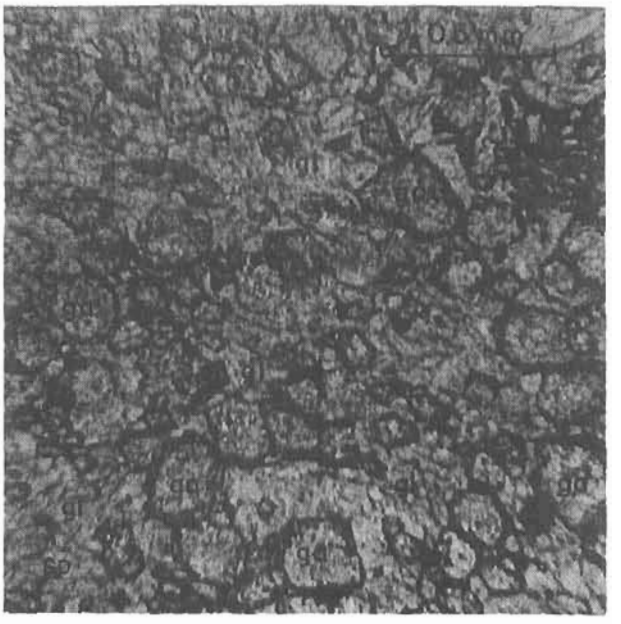

Figure 3. Photomicrograph of garnet-glaucophane metabasite. ga - garnet, gl - glaucophane, sp - sphene.

mineral assemblage is evidence that the earliest metamorphism to affect the schist belt was of the blueschist facies.

Garnet, which makes up from 10 to 60 percent of these rocks, occurs as pinkish-brown porphyroblasts ranging from 0.1 to 1.5 mm in diameter (fig. 3, cover photograph) and commonly exhibits irregular, chlorite-filled fractures. Garnet exhibits all degrees of retrograde metamorphism, from thin chlorite jackets to small islands of garnet that have been completely en-

Table 1. *Chemical analyses (in weight-percent) of metaigneous rocks on Ruby Ridge (USGS rapid-rock analyses).*

	Metafelsite		Metabasite		
	Sample 73RR19f (Locality 1)	Sample 73RR20-3 (Locality 2)	Sample 73RR63f (Locality 3)	Sample 73RR1c[1] (Locality 4)	Sample 73RR52[1] (Locality 5)
SiO_2	70.3	72.1	47.4	50.7	49.6
Al_2O_3	13.5	14.0	16.0	13.2	13.5
Fe_2O_3	1.4	0.68	1.9	4.5	3.3
FeO	2.4	0.84	9.4	9.4	12.2
MgO	2.5	0.67	7.1	6.1	5.5
CaO	0.23	0.51	8.1	9.6	6.7
Na_2O	1.2	1.1	3.3	3.3	2.5
K_2O	5.9	7.0	0.12	0.52	0.06
H_2O+	1.6	0.97	3.2	0.93	1.7
H_2O-	0.11	0.09	0.18	0.00	0.09
TiO_2	0.52	0.42	1.7	1.6	3.7
P_2O_5	0.15	0.09	0.23	0.15	0.39
MnO	0.02	0.00	0.14	0.17	0.21
CO_2	0.02	0.08	1.0	0.33	0.56

[1]Contains glaucophane.

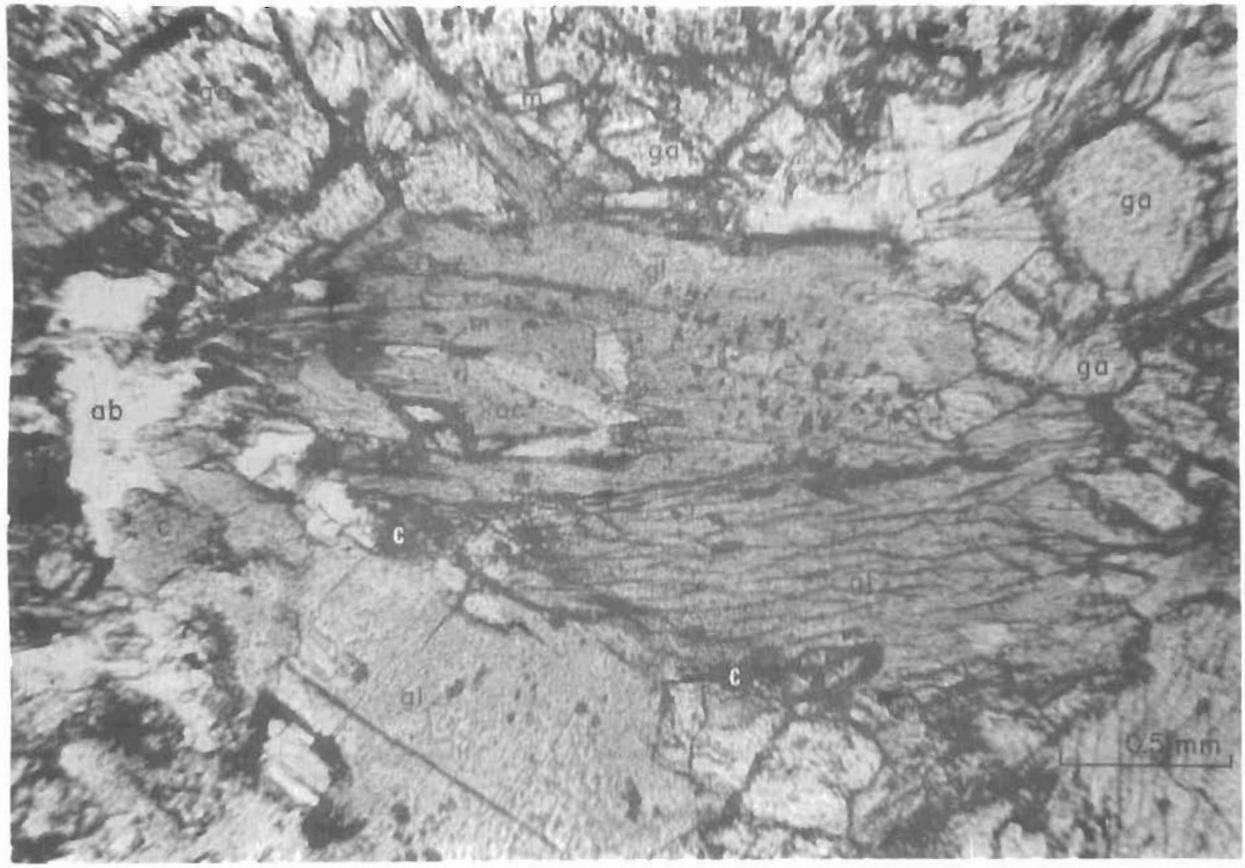

Figure 4. Photomicrograph of retrograded glaucophane-bearing metabasite. Actinolite (ac) is replacing glaucophane (gl). ga - garnet, ab - albite, c - chlorite, m - muscovite.

gulfed by chlorite.

Glaucophane (determined by X-ray diffraction) typically occurs as large pleochroic porphyroblasts up to 3 mm long. The glaucophane most frequently forms a directionless mosaic of decussate, subidioblastic prismatic crystals that surround garnet (fig. 3). Retrograde effects in glaucophane include the appearance of both mottled zones, in which the usual blue pleochroism gives way to the wholesale replacement by actinolite, and felted aggregates of chlorite and actinolite on grain margins (fig. 4). Actinolite does not appear to be in equilibrium with glaucophane, but rather is replacing it.

Epidote is the dominant epidote-family mineral in the glaucophane-bearing rocks, and commonly displays zoning from iron-rich cores to iron-poor rims. One sample contains both epidote and clinozoisite, but the clinozoisite most likely formed later during overprinting by the greenschist-facies metamorphic event.

Sphene is present as a ubiquitous accessory phase and occurs as small idioblastic grains less than 0.1 mm long and in aggregates as large as 2.0 mm across (fig. 3). Rutile commonly occurs as cores in sphene euhedra, which appear to have retrograded to sphene during the greenschist thermal event.

White mica was determined to be paragonite on the basis of its low potassium content. Most of the chlorite found in these rocks has been produced by retrograde metamorphism; however, a small portion may have been in equilibrium with the initial blueschist assemblage.

Trace to minor amounts of quartz and albite are present in some specimens and appear to be the earliest formed minerals. Therefore, this albite formed earlier than that in the felsic schists.

Coarse-grained jadeite occurs in metabasite at one locality on the south slope of VABM Ruby (pl. 1). Jadeite and glaucophane in this rock are cut by a later foliation. Jadeite may have been more common in metabasite prior to greenschist facies overprinting.

GREENSCHIST

Metabasite with greenschist-facies mineralogy is light grayish green to dark olive green on fresh surfaces and varies from massive, fine-grained greenstone to foliated, medium-grained greenstone. The dominant minerals in these rocks are actinolite, epidote, albite, chlorite, and commonly garnet (fig. 5).

Actinolite typically occurs as pleochroic porphyro-

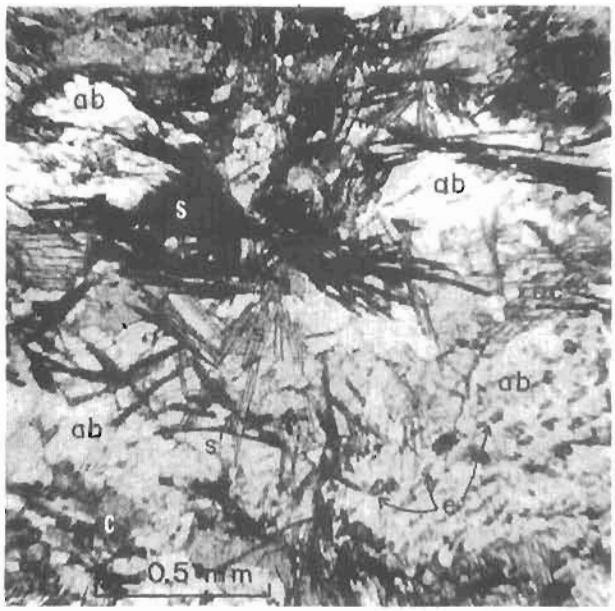

Figure 5. Photomicrograph of greenschist metabasite. ab - albite, s - stilpnomelane, c - chlorite, e - epidote.

blasts, or as a felty aggregate that accounts for 20 to 60 percent of the rock.

Epidote or clinozoisite typically occurs as idioblastic to subidioblastic prisms 0.1-1.0 mm long elongated along their b axis and parallel to the plane of foliation. As in glaucophane-bearing metabasite, epidote is generally zoned from iron-rich cores to iron-poor rims. The zoning is thought to be due to the increase in crystallization temperature associated with greenschist-facies metamorphism that affected earlier formed epidote.

Two generations of garnet are recognized in these rocks: (1) that formed during the blueschist facies metamorphic event, which is retrograded and occurs as small xenoblasts surrounded by chlorite (fig. 6), and (2) that formed during the subsequent greenschist-facies event, which occurs as idioblastic porphyroblasts and is not altered to chlorite.

Albite is present as helicitic untwinned xenoblasts up to 1.5 mm in diameter. Weakly pelochroic chlorite occurs as interstitial laths and aggregates located between larger amphibole, clinozoisite, and garnet grains.

Minor minerals commonly present in these rocks are sphene, quartz, calcite, stilpnomelane (fig. 5) and biotite. Sphene is the most common nonopaque accessory mineral and occurs as euhedral grains, in trains, or as aggregates. Quartz occurs as early-formed, clear, equant, or lenticular grains, whereas sphene and calcite formed late in the paragenesis of these rocks. Rare stilpnomelane occurs as radiating aggregates associated with calcite on the south part of Ruby Ridge, and incipient biotite is seen forming from chlorite in a few samples from the north end of the ridge.

In most cases, greenschist-facies metabasite was previously metamorphosed to high-temperature blueschist facies, although it is difficult to distinguish rocks that are retrograded blueschists from greenschist-facies metabasite formed directly from gabbro or basalt. In many specimens, however, there is excellent textural and mineralogical evidence for formation of greenschists from blueschists (fig. 4). The absence of biotite in blueschist-facies rocks is diagnostic, as previously noted by Taylor and Coleman (1968). However, on the north end of Ruby Ridge, where greenschist-facies metamorphism was most intense, biotite appears as a stable phase in synkinematic assemblages.

The first minerals to be attacked by the retrograde metamorphism are glaucophane and garnet. Glaucophane is usually replaced by a pale-green amphibole that mimics original glaucophane textures (fig. 4). Garnet alters to chlorite, which forms pseudomorphic aggregates after the original porphyroblasts (fig. 6). Epidote in some of the blueschist assemblages has undergone a more subtle transition. South of VABM Ruby epidote grains are commonly zoned from iron-rich cores to iron-poor rims (clinozoisite in many instances). North of peak 3870 clinozoisite is the stable epidote mineral and is usually found as large porphyroblasts. Epidote rarely occurs as inclusions in garnet or albite.

METAFELSITE

Two east-trending bands of felsic schist are present just north and northeast of VABM Ruby (pl. 1). The occurrences are separated by intervening pelitic schist, metabasite, and a thrust fault. The northern felsic schist was probably once laterally continuous with the southern sequence. Most felsic schist is light gray on both fresh and weathered surfaces and forms low angular ridges to subdued and rounded outcrops mantled with slabby talus. A distinctive feature of some outcrops is the presence of slightly elongate, curved slabs and prisms of rock that resemble the sinuous columnar-jointing characteristics of small felsic volcanic domes. The felsic schist commonly contains quartz $\pm$ microcline + muscovite-phengite $\pm$ biotite + albite $\pm$ talc(?) $\pm$ chlorite $\pm$ clinozoisite-epidote + sphene + apatite $\pm$ zircon $\pm$ calcite. Biotite or microcline or both are characteristic of this schist. When present, microcline appears to be recrystallized premetamorphic K-feldspar phenocrysts. The microcline crystals are often euhedral or are angular fragments of euhedral crystals, and deep sinuous embayments randomly penetrate the megacrysts. Some specimens show foliation bending around microcline, while in a few cases foliation seems little altered by the presence of megacrysts 1.5-2.0 cm across. Some intervals are markedly blastoporphyritic with megacrysts of partially resorbed bluish quartz as well as K-feldspar. Except for anhedral form and smaller size, quartz megacrysts closely resemble microcline megacrysts. The quartz and microcline megacrysts

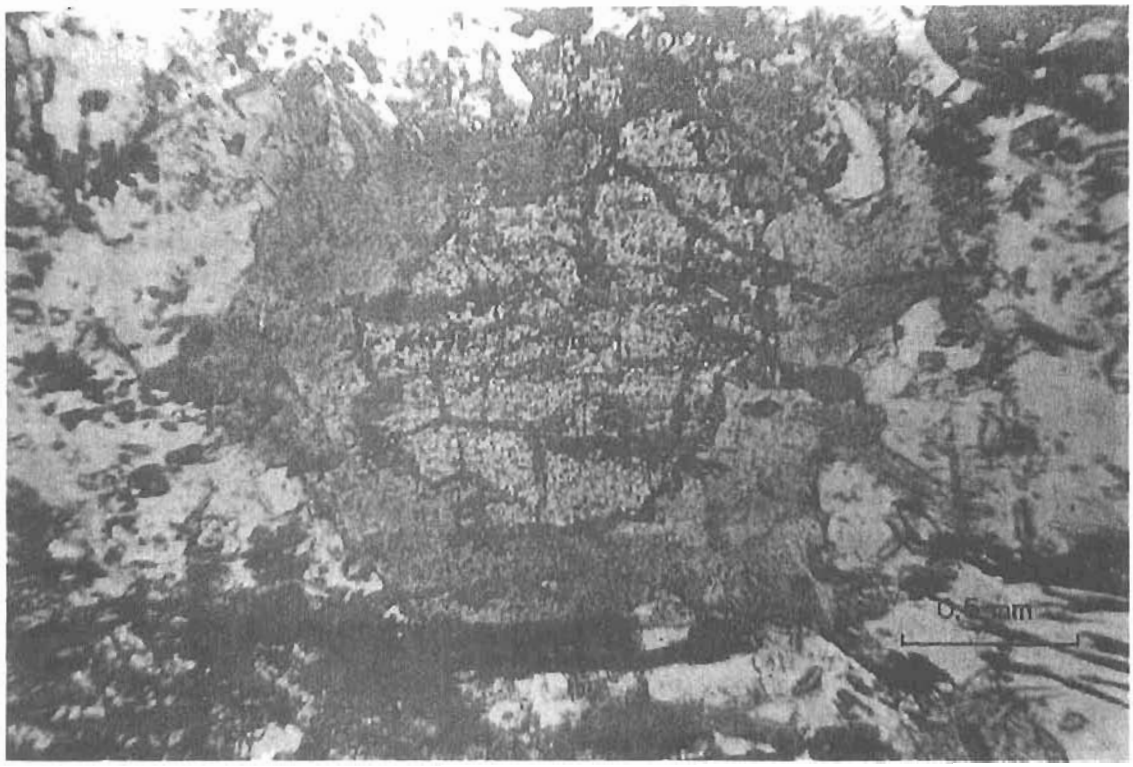

Figure 6. Photomicrograph of greenschist metabasite showing chlorite (c) forming from garnet (ga).

are most likely relict phenocrysts of quartz and K-feldspar, which suggests that the metafelsites were originally felsic hypabyssal or volcanic rocks.

Near VABM Ruby fine-grained brown biotite is usually present as a minor accessory (1-3 percent). These rocks have bulk compositions analogous to potassic rhyolite or granite (table 1). Incipient biotite is also found in pelitic schist adjacent to these units, and it is possible that these two occurrences of biotite are related. Carden and Forbes believe that the metafelsites are synkinematic hypabyssal rocks that were emplaced during a younger metamorphic event, carrying their own thermal perturbation with them at the time of intrusion. The incipient biotite in the adjacent rocks would then be related to hornfelsing at the time of intrusion. Wiltse and Gilbert believe that the metafelsite constitutes a metamorphosed submarine volcanic sequence of felsic lavas and tuffs. Wiltse (1975) postulated that the biotite in the schist surrounding the most quartzose feldspathic units was due to the high potassium content of metamorphosed pelitic sediments that had incorporated tuffaceous volcanic debris. This view rejects any significant hornfelsing.

Porphyroblasts of albite are rare in the metafelsite and are paragenetically late. Epidote and calcite occasionally occur in rocks containing albite. Sphene, apatite, and zircon are present in trace amounts. A few felsic schists contain 1-2 percent pyrite in 6- to 12-mm-wide cubes.

SOUTHWESTERN END OF RUBY RIDGE

On the southwestern end of Ruby Ridge near peak 2100 is a sequence of massive, weakly metamorphosed greenstone and thinly bedded, fine-grained gray marble. Intercalated with these rocks are minor amounts of phyllite, calc-phyllite, and black chert. These rocks strike approximately east-west and dip south under the Ambler Lowland.

The greenstone, which makes up 60 percent of the rocks near peak 2100, is very thickly layered and displays schistosity only along widely spaced shear surfaces. In thin section a relict igneous mineralogy and texture is preserved. Some samples have a tuffaceous texture. The greenstone contains relict primary plagioclase, pyroxene, and glass, which are commonly altered to epidote and chlorite. These rocks probably were metamorphosed in the prehnite-pumpellyite facies or lowest part of the greenschist facies.

Marble, which makes up 30 percent of the rocks near peak 2100, is thin, flaggy, and very weakly metamorphosed (fig. 7). Fine-grained calcite is the dominant mineral phase, and there are minor amounts of quartz and sericite.

Medium- to dark-gray phyllite and calc-phyllite crop out on Ruby Ridge near peak 2060. These rocks are composed dominantly of quartz, sericite, and plagioclase. Some specimens contain enough calcite to freely effervese in dilute hydrochloric acid.

Figure 7. Photograph of south-dipping marble 0.6 km west of peak 2100 on southwestern end of Ruby Ridge.

STRUCTURE

INTRODUCTION

The structure of rocks on Ruby Ridge reflects at least two episodes of dynamic metamorphism and penetrative deformation. These events were superimposed on a preexisting basement terrane metamorphosed, in part, to blueschist facies. At only one locality were dynamic features formed during the early, blueschist metamorphic event observed, but it is likely that early dynamic features are largely masked by later events. The first noticeable major dynamic event generated recumbent folds, thrust faults, and crystallization foliation. The second dynamic event generated open to subisoclinal folds and slip cleavage, but was not accompanied by extensive recrystallization.

EARLY ISOCLINAL FOLDS AND THRUST FAULTS

The first dynamic event is characterized by isoclinal to subisoclinal folds (F_1) overturned to the north (fig. 8) and is accompanied by synkinematic recrystallization and segregation of metasedimentary rocks into mica-rich and quartz-rich layers (S_1). Earlier S_0 layering is generally transposed and parallel to S_1 foliation. Isoclinal- and subisoclinal-fold wavelengths vary from microscopic to several hundred meters. Near peak 3870 is a tectonically thickened zone where numerous recumbent folds are piled on one another (fig. 9). This zone of thickening, or protonappe development, probably reflects movement northward. Large isoclinal folds are also present 2.0 km north and south of VABM Ruby along Ruby Ridge.

The northwest-trending overturned antiform and synform on the north end of Ruby Ridge were probably formed at the same time as the isoclinal folds to the south. These folds are less closed than isoclinal folds to the south, and suggest that F_1 deformation was less intense to the north.

Scattered F_1 fold axes suggest an east-west trend for F_1 folds (fig. 10). However, S_1 foliation on both the north and south limbs of the Kalurivik Arch defines vague girdles that most likely are due to variable limbs of F_1 folds, especially in the zone of tectonic thickening (pl. 1, fig. 11a-c). F_1 fold axes calculated from both girdles were rotated by unfolding the Kalurivik Arch and suggest a prearch F_1 trend of N. 72° W. and a plunge of 16° (fig. 11a,b).

Thrust faults associated with subisoclinal-isoclinal

Figure 8. Isoclinal F_1 folds near VABM Ruby.

folds are present near VABM Ruby, and probably occur elsewhere, especially near peak 3870. The thrust surfaces are not conspicuous and are discovered only by detailed mapping of adjacent lithologic units (fig. 12). The two thrust faults north of VABM Ruby dip south about 35°, subparallel to S_1. Displacements along these faults is unknown, but are probably tens to hundreds of meters. An overturned antiform and synform are present just beneath the eastern part of the upper thrust fault.

The Walker Lake fault mapped to the east (Pessel and others, 1973b) projects toward the north end of Ruby Ridge (pl. 1), but no evidence of this fault was observed. The Walker Lake fault may be present on Ruby Ridge, juxtaposing similar rock types, or it may merge into a fold system along strike.

LATER FOLDS AND FORMATION OF KALURIVIK ARCH

A later, primarily dynamic metamorphic event also affected the Ruby Ridge area. This event is characterized by open to subisoclinal folds (F_2) ranging from microscopic crenulations to folds with wavelengths of several meters. These folds are present all along the ridge, but appear slightly more intense to the north. F_2 fold axes trend approximately east-west, with a preferred orientation of S. 78° E. and a plunge of 8° (fig. 13).

A slip cleavage (S_2) is commonly developed parallel to F_2 axial surfaces and dips gently northward (fig. 14). This cleavage is well developed north of the Kalurivik

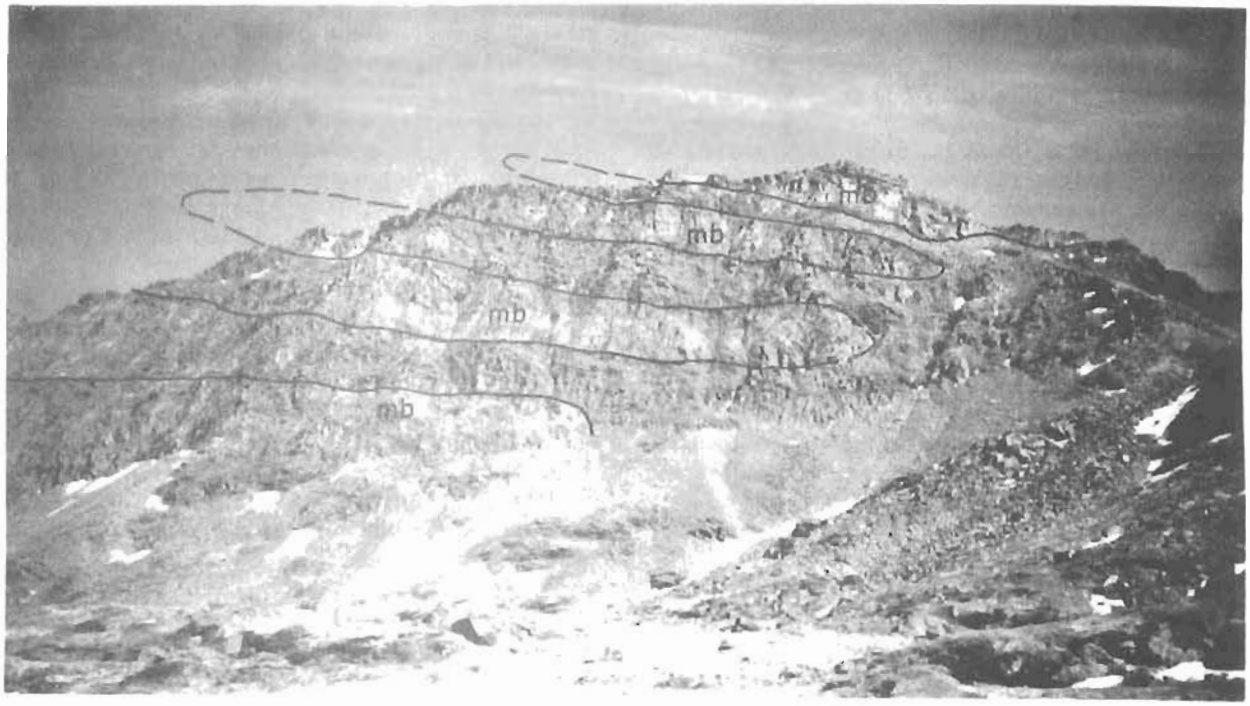

Figure 9. Recumbent isoclinal folds on cliff west of peak 3870. mb - metabasite.

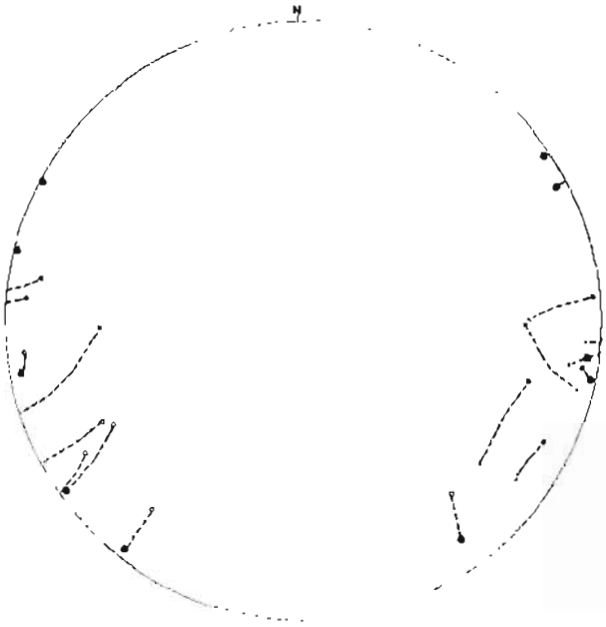

Figure 10. Lower hemisphere equal-area plot of 17 F_1 fold axes. x - from north of Kalurivik Arch. o - from south of Kalurivik Arch. Prearch orientation determined by rotating attitude to horizontal. ⊕ - prearch F_1 orientation north of Kalurivik Arch, ● = prearch F_1 orientation south of Kalurivik Arch.

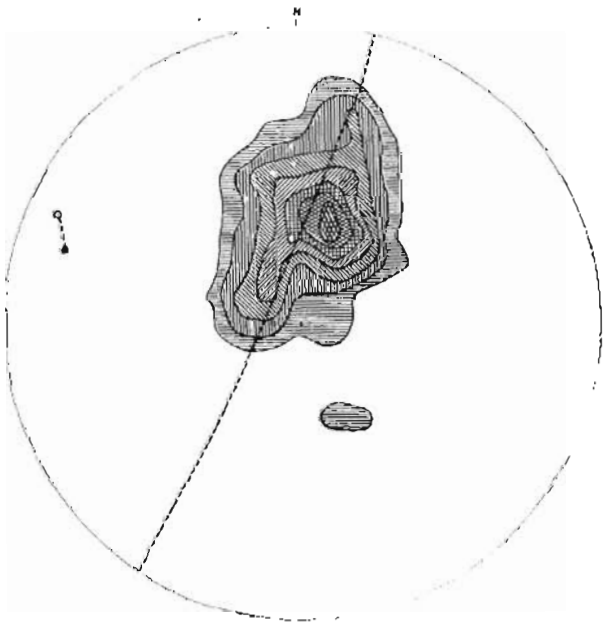

Figure 11b. Lower hemisphere equal-area plot of 127 poles to S_1 foliation south of Kalurivik Arch along Ruby Ridge. Contour interval at 2, 4, 6, 8, 10, 12, and 14 percent per 1-percent area. General F_1 fold axis (open circle) calculated from vague girdle lying along dashed small circle. ● - general prearch F_1 fold axis determined by rotating Kalurivik Arch to horizontal.

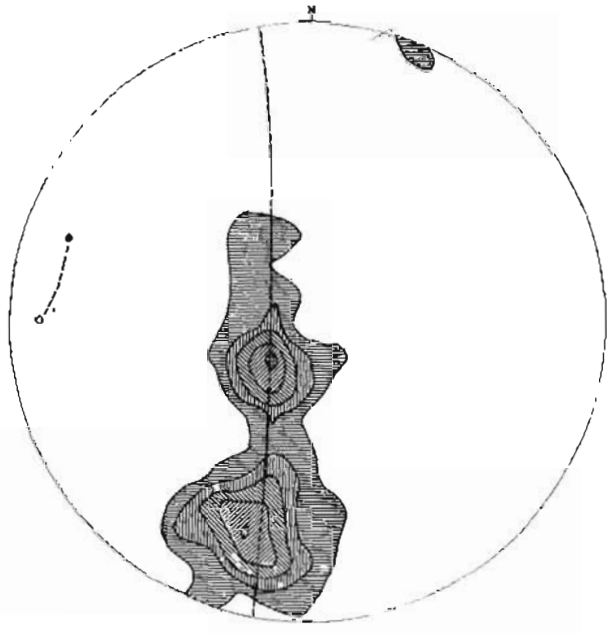

Figure 11a. Lower hemisphere equal-area plot of 167 poles to S_1 foliation north of Kalurivik Arch along Ruby Ridge. Contour interval at 2, 4, 6, 8, and 10 percent per 1-percent area. General F_1 fold axis (open circle) calculated from vague girdle lying along dashed small circle. ● - general prearch F_1 fold axis determined by rotating Kalurivik Arch to horizontal.

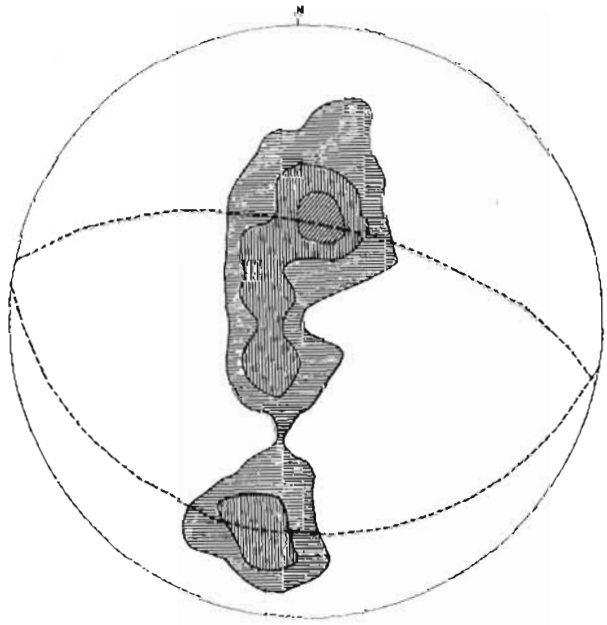

Figure 11c. Lower hemisphere equal-area plot of 294 poles to S_1 foliation along Ruby Ridge. Contour interval at 2, 4, and 6 percent per 1-percent area. Dashed lines are general trace of north and south limbs of Kalurivik Arch calculated from π diagram. Intersection of trace of limbs = calculated axis of Kalurivik Arch.

Figure 12. Trace of thrust fault on ridge northeast of VABM Ruby

Figure 13. Lower hemisphere equal-area plot of 75 F_2 fold axes along Ruby Ridge. Contour interval at 4, 8, 12, and 16 percent per 1-percent area.

Figure 14. Lower hemisphere equal-area plot of 38 poles to S_2 cleavage. • - from north of Kalurivik Arch. x - from south of Kalurivik Arch.

Arch, while south of the arch it is commonly incipient (fig. 15).

The Kalurivik Arch is an antiform that extends for at least 62 km along the schist belt (Pessel and Brosge, 1977). Near Ruby Ridge the Kalurivik Arch is asymmetrical, deflecting major lithologic units (S_1) moderately to the south and steeply to the north (fig. 11c). The arch may have formed at about the same time as the F_2 fold event, since the calculated axis of the arch (fig. 11c) is nearly identical with the axes of F_2 folds (fig. 13). On the other hand, S_2 cleavage is not affected by the arch and could have formed synchronous with or following the arching.

High-angle faults mapped in several places formed either during the last major dynamic event or later. On the north end of Ruby Ridge a northwest-trending high-angle fault truncates a marble interval and a greenstone interval. Just north of peak 3870 a probable high-angle fault marks a major inflection of the Kalurivik Arch (pl. 1). Just north of VABM Ruby several high-angle faults truncate lithologic intervals (pl. 1). The direction of movement and displacement along these faults is unknown, but is likely a few tens of meters. Similar faults are undoubtedly present elsewhere along Ruby Ridge.

AEROMAGNETIC SURVEY

Total-intensity magnetic data from the 1975 Alaska DGGS aeromagnetic survey (flown by Geometrics, Inc.) were obtained with a continuous digital-recording proton magnetometer installed in a twin-engine fixed-wing aircraft. Flight paths were north-south, about 1.2 km apart, 330 m above ground level. Total magnetic intensity anomaly values over the study area vary from -150 gammas in the Ambler Lowland to +450 gammas in the Schwatka Mountains (fig. 16). Extensive linear zones of high intensity lie over the Cosmos Hills and the uplands of the Baird and Schwatka Mountains. Broad east-west magnetic lows and highs occur over the southern portions of the schist belt. Flat magnetic lows occur over the majority of the Ambler Lowland. The dominant west-northwest regional magnetic trends are locally deflected by northwest-southeast structural features suggestive of transcurrent block movements (fig. 16). Magnetic features are not appreciably influenced by topography and are superimposed on a negative southwestward regional gradient of about 2.7 gammas/km. If remanent magnetization is present, body size, shape, and dip and magnetization direction are inseparable until rock susceptibility values are determined.

In the Cosmos Hills are a sharp, high-amplitude magnetic signature associated with serpentinite, metaconglomerate, and metabasalt, and moderate to broad magnetic highs and lows associated with phyllite (fig. 16). Metamorphic and volcanic rocks of the schist belt have a subdued and variable magnetic response but show a strongly developed regional magnetic strike parallel to tectonic trends (fig. 16).

A conspicuous feature in the study area is the lack of magnetic anomalies greater than 40 gammas over the southern Brooks Range copper deposits. Truncation of magnetic anomalies suggest major basement faults or near vertical contacts at depth between the Cosmos Hills and the schist belt. In addition, a major change in magnetic gradient indicates a contrast in basement lithology along the south margin of the schist belt (fig. 16). Superimposed on these magnetic features is a linear zone of nearly flat gradient that reflects the major topographic depression of the Ambler Lowland.

The geologic and geophysical contrasts between the schist belt and Ambler Lowland-Cosmos Hills area suggest that a major tectonic boundary just north and parallel to the Ambler Lowland may juxtapose the weakly metamorphosed Paleozoic basalt and carbonate terrane to the south against polymetamorphic Precambrian and younger(?) rocks of the schist belt to the north (fig. 17). If such a tectonic boundary exists, it probably crosses Ruby Ridge 3.5 km southwest of VABM Ruby.

A narrow magnetic high is associated with the Walker Lake lineament (Fritts and others, 1972) and trends from Walker Lake in the east to where it broadens westward near the Redstone River and truncates against the

Figure 15. Photograph of F_2 folds and S_2 cleavage (parallel to hammerhead).

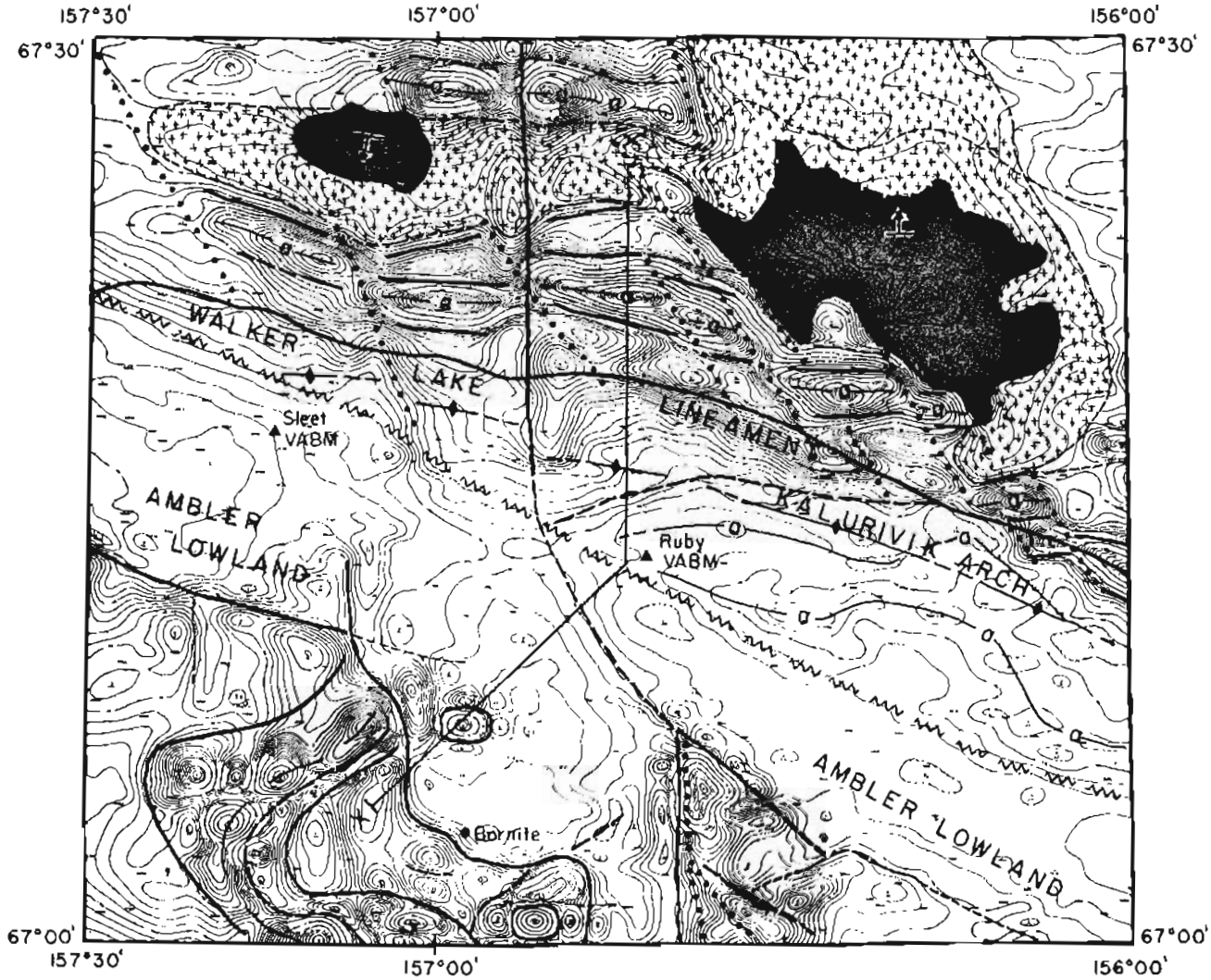

EXPLANATION

Granitic intrusion, showing apparent dip

Area of large broad aeromagnetic low indicating presences of granitic intrusive rock

Principal magnetic boundary

Subordinate magnetic boundary

Subdued magnetic boundary

Regional magnetic discontinuity

Termination or break in magnetic anomaly trend, probably caused by basement faulting

Alignment of selected magnetic highs & lows

Schematic structure section & aeromagnetic profile shown in fig. 17

MAGNETIC DATA

Contour interval. . . . . .10 gammas

Datum. . . . . .56,380 gammas

Flight line spacing. . . . . 1.0 miles

Flight altitude. . . . . .1,000 feet AGL

Magnetic declination. . . . . .23°

Magnetic inclination. . . . . .77°

A regional trend of 3.46 gammas/mile North & 2.25 gammas/mile East was removed using the 1965 IGRF updated to 1974

Flown & processed by Geometrics 1974-76

N

0 5 MILES

0 5 10 KILOMETERS

Figure 16. Regional aeromagnetic features of area covered by fig. 1.

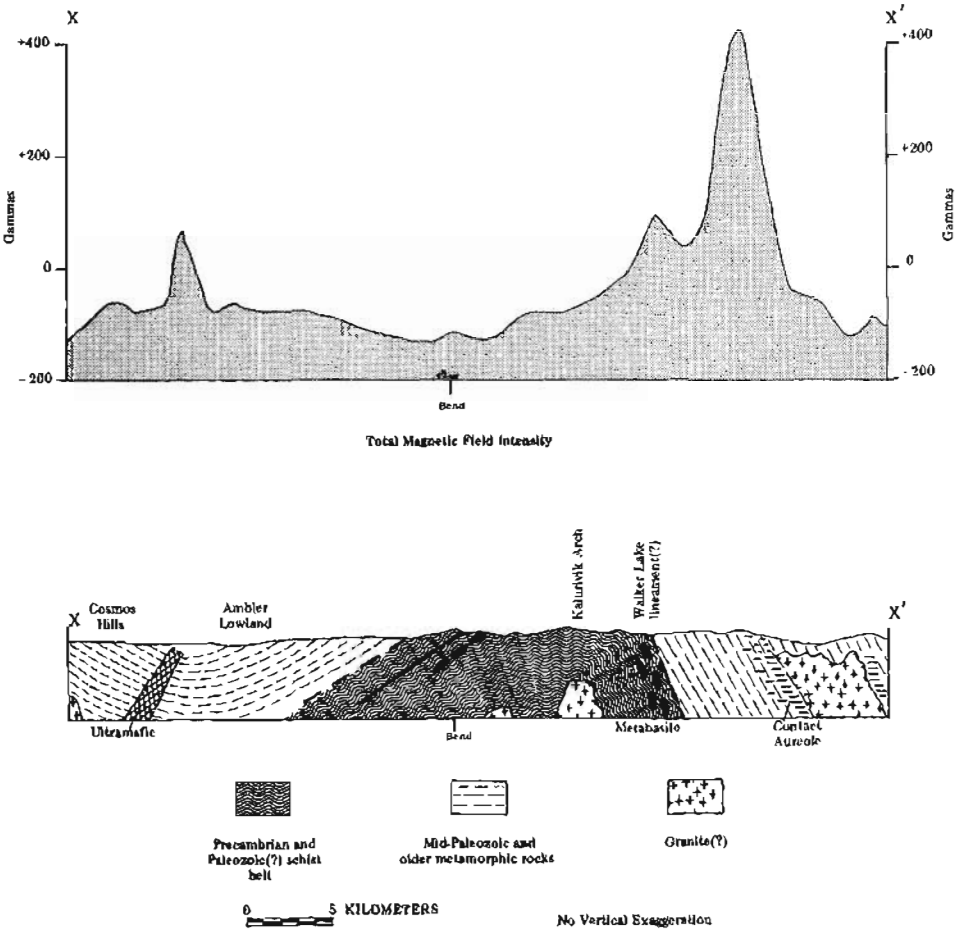

Figure 17. Schematic geologic cross section and aeromagnetic profile along X-X' of fig. 1.

major change in magnetic gradient just described. Where the Walker Lake lineament has a sharply defined magnetic signature to the east, it appears to be a thrust fault. The broadening and curved nature of this signature near Ruby Ridge corresponds with the north-verging overturned antiform and synform on the north end of Ruby Ridge.

The Redstone and Shishakshinovick plutons are characterized by low-amplitude magnetic anomalies (fig. 16). Contact metamorphic effects have produced magnetic aureoles adjacent to and within the Paleozoic basement that outline the southern margins of the intrusions. Magnetic patterns and configurations indicate a north dip for the Shishakshinovick pluton and a south dip for the Redstone pluton.

TECTONIC SUMMARY

The geology of Ruby Ridge suggests that most of the rocks in the southern Brooks Range schist belt were once shallow-marine sedimentary and mafic volcanic rocks of Precambrian age. During late Precambrian time these rocks were metamorphosed in the blueschist facies and converted into continental basement. Wiltse and Gilbert believe that a felsic volcanic assemblage, which included marine pelite and carbonate, was deposited unconformably on Precambrian basement during mid-Paleozoic time (Wiltse and Gilbert, 1977) and may represent magmatism associated with Brooks Range mid-Paleozoic orogeny. All authors of this paper believe that some Phanerozoic rocks are probably now tectonically intercalated with Precambrian rocks.

During Jurassic-Cretaceous time the schist-belt basement probably impinged against the Paleozoic Cosmos Hills-Angayucham terrane. The thrust faulting, isoclinal folding, and regional greenschist-facies metamorphism seen on Ruby Ridge are likely only a small part of widespread Cretaceous tectonism and plutonism that affected the western Brooks Range (Tailleur and Brosge, 1970; Tailleur, 1973; Newman and others, 1977) and may be the deep-seated manifestation of deformational events that moved overlying Paleozoic assemblages northward to form the major nappe structures in the central part of the western Brooks Range (fig. 17).

During Late Cretaceous or Tertiary time the schist belt was again folded and perhaps uplifted along the trend of the Kalurivik Arch. The belt probably formed a structural high from which almost all overlying rocks have been tectonically stripped or removed by erosion.

Aeromagnetic evidence (fig. 16) suggests that the tectonic boundary between the Cosmos Hills-Angayucham terrane and the schist belt was reactivated as a strike-slip system during Tertiary time. Right-lateral movement along this zone may have caused readjustment of older rocks along secondary faults.

ACKNOWLEDGMENTS

The authors wish to thank I.L. Tailleur, W.P. Brosge, C.F. Mayfield, and G.H. Pessel for many stimulating discussions of southern Brooks Range geology. Tailleur, Mayfield, and J.T. Dillon provided helpful reviews of the manuscript, and J.T. Kline, M.W. Henning, and J.W. Buza assisted field parties during 1975. The authors also wish to thank the U.S. Geological Survey, Bear Creek Mining Company and Sunshine Mining Company for their assistance and cooperation with this study.

This research was partly supported by National Scenic Foundation grant GA 43004. Carden is also grateful for support from a Geological Society of America Penrose bequest grant and a Sigma Xi grant in aid of research.

REFERENCES CITED

Brosge, W.P., and Pessel, G.H., 1977. Preliminary reconnaissance geologic map of the Survey Pass quadrangle, Alaska: U.S. Geol. Survey Open-File Rept. 77-27.

Forbes, R.B., Turner, D.L., Gilbert, W.G., and Carden, J.R., 1974, Ruby Ridge traverse, southwestern Brooks Range: Alaska Div. Geol. and Geophys. Surveys 1973 Ann. Rept., p. 34-36.

Fritts, C.E., 1969, Geology and geochemistry in the southeastern part of the Cosmos Hills, Shungnak D-2 quadrangle, Alaska: Alaska Div. Mines and Geol. Geol. Rept. 37, 35 p., map.

_____, 1970, Geology and geochemistry of the Cosmos Hills, Ambler River and Shungnak quadrangles, Alaska: Alaska Div. Mines and Geol. Geol. Rept. 39, 69 p., map.

_____, 1971, Geology and geochemistry of the Angayucham Mountains, western Alaska: Alaska Div. of Geol. Survey 1970 Ann. Rept., p. 1-8, 1-9.

Fritts, C.E., Eakins, G.R., and Garland, R.E., 1972, Geology and geochemistry near Walker Lake, southern Survey Pass quadrangle, arctic Alaska: Alaska Div. Geol. Survey 1971 Ann. Rept., p. 19-26.

Mayfield, C.F., 1975, Metamorphism in southwestern Brooks Range: Geological Survey Research 1975, U.S. Geol. Survey Prof. Paper 975, p. 64-65.

Newman, G.W., Mull, C.G., and Watkins, N.D., 1977, Northern Alaska paleomagnetism, plate rotation, and tectonics, *in* The relationship of plate tectonics to Alaska geology and resources: Alaska Geol. Soc. Symposium, 1977, Anchorage, AK, p. 16-19.

Patton, W.W., Jr., Miller, T.P., and Tailleur, I.L., 1968, Regional geologic map of the Shungnak and southern part of the Ambler River quadrangle, Alaska: U.S. Geol. Survey Misc. Geol. Inv. Map I-554.

Patton, W.W., Jr., and Miller, T.P., 1973, Bedrock geologic map of Bettles and southern part of Wiseman quadrangle, Alaska: U.S. Geol. Survey Mineral Inv. Map MF-492.

Pessel, G.H., Eakins, G.R., and Garland, R.E., 1973a, Geology and geochemistry of the southeastern Ambler River quadrangle, *in* Alaska Div. Geol. and Geophy. Surveys 1972 Ann. Rept., p. 7-8.

Pessel, G.H., Garland, R.E., Tailleur, I.L., and Eakins, G.R., 1973b, Preliminary geologic map of southeastern Ambler River and part of Survey Pass quadrangle, Alaska: Alaska Div. Geol. and Geophys. Surveys Open-File Rept. 36.

Pessel, G.H., and Brosge, W.P., 1977, Preliminary reconnaissance geologic map of Ambler River quadrangle, Alaska: U.S. Geol. Survey Open-File Rept. 77-28.

Tailleur, I.L., and Brosge, W.P., 1970, Tectonic history of northern Alaska, *in* Proceedings of the geological seminar on the north slope of Alaska: Los Angeles, Pacific Sec., Am. Assoc. Petroleum Geologists, p. E1-E19.

Tailleur, I.L., 1973, Probable rift origin of the Canada Basin, Arctic Ocean, *in* Arctic geology (M.G. Pitcher, ed.): Am. Assoc. Petroleum Geologists Mem. 19, p. 526-535.

Taylor, H.P., and Coleman, R.G., 1968, O^{18}/O^{16} ratios of co-existing minerals in glaucophane-bearing metamorphic rocks: Geol. Soc. America Bull., v. 79, p. 1727-1756.

Turner, D.L., 1974, Geochronology of southwestern Brooks Range metamorphic rocks: Alaska Div. Geol. and Geophys. Surveys 1973 Ann. Rept., p. 27-30.

Turner, D.L., and Forbes, R.B., 1977, Geochronology of the southwestern Brooks Range, *in* The relationship of plate tectonics to Alaskan geology and resources: Alaska Geol. Soc. Symposium, 1977, Anchorage, AK, p. 42-43.

Wiltse, M.A., 1975, Geology of the Arctic Camp prospect, Ambler River quadrangle, Alaska: Alaska Div. Geol. and Geophys. Surveys Open-File Rept. 60.

Wiltse, M.A., and Gilbert, W.G., 1977, Regional setting of southern Brooks Range copper deposits, Alaska: Geol. Assoc. Canada Annual Meeting, 1977, Vancouver, B.C., Prog. with Abs., v. 2, p. 55.

dominant foliation (S_1); it rarely occurs as bodies up to several meters thick that cut across the dominant foliation. Exposures range from massive, jointed, angular outcrops surrounded by large, blocky boulders to well-foliated, schistose-slabby outcrops. The metabasite interval on the crest of Ruby Ridge 1.7 km north of VABM 3870 has pillow structures. The parent material of the metabasite probably consisted of basalt flows and gabbroic intrusions (table 1).

There is a continuous variation between massive, coarse-grained, glaucophane-bearing metabasite and occasionally foliated, fine- to medium-grained greenstone with greenschist-facies mineral assemblages (figs. 3, 4, and 5), but the two end members will be described separately.

GLAUCOPHANE-BEARING METABASITE

These rocks are generally massive with no apparent schistosity and form prominent ridges (fig. 2). Fresh samples are blue to bluish green, with a coarse-grained, poikioblastic granular texture highlighted by reddish-brown garnets that stand out in relief on weathered surfaces. The absence of schistosity, which is unusual for glaucophane schist, appears to be due to the lack of penetrative deformation. However, a crude foliation was observed in a few partially retrograded rocks and appears to be defined by minerals such as chlorite, actinolite, and white mica that crystallized during the later greenschist-facies event. A notable exception is a metabasite near the axis of the Kalurivik Arch that has a well-defined schistosity defined by the parallel alignment of subidioblastic glaucophane prisms.

The main metamorphic minerals present in glaucophane-bearing metabasite are garnet, glaucophane, epidote, sphene, rutile, chlorite, and white mica. This

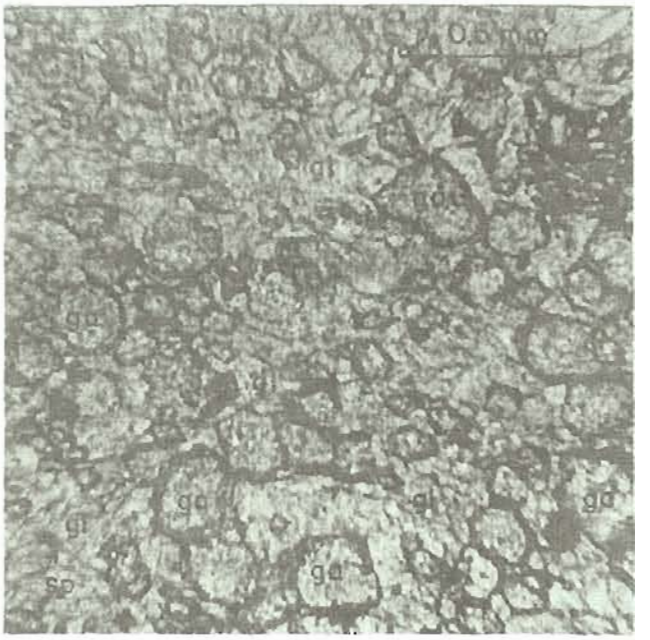

Figure 3. Photomicrograph of garnet-glaucophane metabasite. ga - garnet, gl - glaucophane, sp - sphene.

mineral assemblage is evidence that the earliest metamorphism to affect the schist belt was of the blueschist facies.

Garnet, which makes up from 10 to 60 percent of these rocks, occurs as pinkish-brown porphyroblasts ranging from 0.1 to 1.5 mm in diameter (fig. 3, cover photograph) and commonly exhibits irregular, chlorite-filled fractures. Garnet exhibits all degrees of retrograde metamorphism, from thin chlorite jackets to small islands of garnet that have been completely en-

Table 1. *Chemical analyses (in weight-percent) of metaigneous rocks on Ruby Ridge (USGS rapid-rock analyses).*

	Metafelsite		Metabasite		
	Sample 73RR19f (Locality 1)	Sample 73RR20-3 (Locality 2)	Sample 73RR63f (Locality 3)	Sample 73RR1c[1] (Locality 4)	Sample 73RR52[1] (Locality 5)
SiO_2	70.3	72.1	47.4	50.7	49.6
Al_2O_3	13.5	14.0	16.0	13.2	13.5
Fe_2O_3	1.4	0.68	1.9	4.5	3.3
FeO	2.4	0.84	9.4	9.4	12.2
MgO	2.5	0.67	7.1	6.1	5.5
CaO	0.23	0.51	8.1	9.6	6.7
Na_2O	1.2	1.1	3.3	3.3	2.5
K_2O	5.9	7.0	0.12	0.52	0.06
H_2O+	1.6	0.97	3.2	0.93	1.7
H_2O-	0.11	0.09	0.18	0.00	0.09
TiO_2	0.52	0.42	1.7	1.6	3.7
P_2O_5	0.15	0.09	0.23	0.15	0.39
MnO	0.02	0.00	0.14	0.17	0.21
CO_2	0.02	0.08	1.0	0.33	0.56

[1]Contains glaucophane.

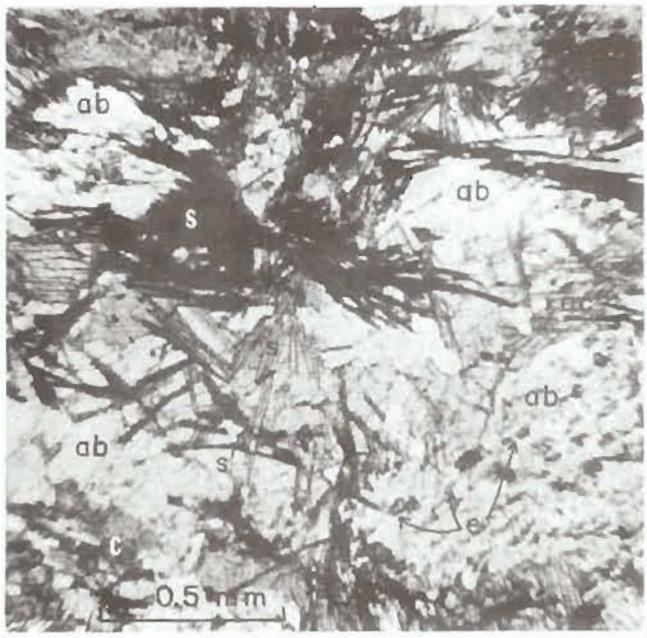

Figure 5. Photomicrograph of greenschist metabasite. ab - albite, s - stilpnomelane, c - chlorite, e - epidote.

blasts, or as a felty aggregate that accounts for 20 to 60 percent of the rock.

Epidote or clinozoisite typically occurs as idioblastic to subidioblastic prisms 0.1-1.0 mm long elongated along their b axis and parallel to the plane of foliation. As in glaucophane-bearing metabasite, epidote is generally zoned from iron-rich cores to iron-poor rims. The zoning is thought to be due to the increase in crystallization temperature associated with greenschist-facies metamorphism that affected earlier formed epidote.

Two generations of garnet are recognized in these rocks: (1) that formed during the blueschist facies metamorphic event, which is retrograded and occurs as small xenoblasts surrounded by chlorite (fig. 6), and (2) that formed during the subsequent greenschist-facies event, which occurs as idioblastic porphyroblasts and is not altered to chlorite.

Albite is present as helicitic untwinned xenoblasts up to 1.5 mm in diameter. Weakly pelochroic chlorite occurs as interstitial laths and aggregates located between larger amphibole, clinozoisite, and garnet grains.

Minor minerals commonly present in these rocks are sphene, quartz, calcite, stilpnomelane (fig. 5) and biotite. Sphene is the most common nonopaque accessory mineral and occurs as euhedral grains, in trains, or as aggregates. Quartz occurs as early-formed, clear, equant, or lenticular grains, whereas sphene and calcite formed late in the paragenesis of these rocks. Rare stilpnomelane occurs as radiating aggregates associated with calcite on the south part of Ruby Ridge, and incipient biotite is seen forming from chlorite in a few samples from the north end of the ridge.

In most cases, greenschist-facies metabasite was previously metamorphosed to high-temperature blueschist facies, although it is difficult to distinguish rocks that are retrograded blueschists from greenschist-facies metabasite formed directly from gabbro or basalt. In many specimens, however, there is excellent textural and mineralogical evidence for formation of greenschists from blueschists (fig. 4). The absence of biotite in blueschist-facies rocks is diagnostic, as previously noted by Taylor and Coleman (1968). However, on the north end of Ruby Ridge, where greenschist-facies metamorphism was most intense, biotite appears as a stable phase in synkinematic assemblages.

The first minerals to be attacked by the retrograde metamorphism are glaucophane and garnet. Glaucophane is usually replaced by a pale-green amphibole that mimics original glaucophane textures (fig. 4). Garnet alters to chlorite, which forms pseudomorphic aggregates after the original porphyroblasts (fig. 6). Epidote in some of the blueschist assemblages has undergone a more subtle transition. South of VABM Ruby epidote grains are commonly zoned from iron-rich cores to iron-poor rims (clinozoisite in many instances). North of peak 3870 clinozoisite is the stable epidote mineral and is usually found as large porphyroblasts. Epidote rarely occurs as inclusions in garnet or albite.

METAFELSITE

Two east-trending bands of felsic schist are present just north and northeast of VABM Ruby (pl. 1). The occurrences are separated by intervening pelitic schist, metabasite, and a thrust fault. The northern felsic schist was probably once laterally continuous with the southern sequence. Most felsic schist is light gray on both fresh and weathered surfaces and forms low angular ridges to subdued and rounded outcrops mantled with slabby talus. A distinctive feature of some outcrops is the presence of slightly elongate, curved slabs and prisms of rock that resemble the sinuous columnar-jointing characteristics of small felsic volcanic domes. The felsic schist commonly contains quartz $\pm$ microcline + muscovite-phengite $\pm$ biotite + albite $\pm$ talc(?) $\pm$ chlorite $\pm$ clinozoisite-epidote + sphene + apatite $\pm$ zircon $\pm$ calcite. Biotite or microcline or both are characteristic of this schist. When present, microcline appears to be recrystallized premetamorphic K-feldspar phenocrysts. The microcline crystals are often euhedral or are angular fragments of euhedral crystals, and deep sinuous embayments randomly penetrate the megacrysts. Some specimens show foliation bending around microcline, while in a few cases foliation seems little altered by the presence of megacrysts 1.5-2.0 cm across. Some intervals are markedly blastoporphyritic with megacrysts of partially resorbed bluish quartz as well as K-feldspar. Except for anhedral form and smaller size, quartz megacrysts closely resemble microcline megacrysts. The quartz and microcline megacrysts